Unraveling the Influence of Six Lupane-, Oleanane-, and Ursane- type Pentacyclic Triterpenes' Structure-Activity Relationship on Non-Small Lung Adenocarcinoma Cells

Anamaris Torres-Sanchez , Grace Torres , Sthephanie Estrada , Daraishka Pérez , Carlos Garcia , Melissa Milian , Eddian Velazquez , Valerie Molina , Yamixa Delgado *

Posted Date: 4 January 2024

doi: 10.20944/preprints202401.0331.v1

Keywords: Pentacyclic triterpenes; Non-small cell lung carcinoma; A549 cells; Flow cytometry

Article

Unraveling the Influence of Six Lupane-, Oleanane-, and Ursane- Type Pentacyclic Triterpenes' Structure-Activity Relationship on Non-Small Lung Adenocarcinoma Cells

Anamaris Torres-Sanchez [1,2], Grace Torres [3], Sthephanie Estrada [4], Daraishka Pérez [3], Carlos García [5], Melissa Milian [3], Eddian Velazquez [3], Valerie Molina [3] and Yamixa Delgado [3,*]

[1] Biology Department, University of Puerto Rico-Rio Piedras, San Juan PR
[2] Biochemistry Department, University of Puerto Rico Medical Sciences Campus, San Juan PR
[3] Biochemistry & Pharmacology Department, San Juan Bautista School of Medicine, Caguas PR
[4] Biology Department, University of Puerto Rico-Cayey, Cayey PR
[5] Medical Program, Ponce Health Science University, Ponce PR
* Correspondence: ydelgado@sanjuanbautista.edu

Abstract: In recent times, a great interest has been motivated in plant-derived compounds known as phytochemicals. The pentacyclic oleanane-, ursane-, lupane-type triterpenes are phytochemicals that exert significant activities against diseases like cancer. Lung cancer is the leading cause of cancer-related death worldwide. Although chemotherapy is the treatment of choice for lung cancer, its effectiveness is hampered by the dose-limiting toxic effects and chemoresistance. Herein, we investigated the structure-activity relationship of six pentacyclic triterpenes: oleanolic acid (OleA), ursolic acid (UrA), asiatic acid (AsA), betulinic acid (BeA), betulin (Betu), lupeol (Lupe), on NSCLC A549 cells. From our studies, we confirmed that all these triterpenes showed cytotoxicity in the mid μM range, where BeA showed the strongest effect. Then, we determined that most of these triterpenes induced S-phase and G2/M phase cycle arrest, reactive oxygen species, mitochondrial depolarization, and caspase 3 activation. For chemoresistance markers, we elucidated that most triterpenes downregulated STAT3 and PDL1 genes. In contrast, ursane-type UrA and AsA also induced DNA damage, reactive nitrogen species and autophagy. These results showed that even slight structural changes in these triterpenes can influence the cellular response and mechanistic pathways. This study opens promising perspectives for further research on the pharmaceutical role of phytochemical triterpenoids.

Keywords: pentacyclic triterpenes; non-small cell lung carcinoma; A549 cells; flow cytometry

1. Introduction

Triterpenes are secondary metabolites abundantly found in numerous plant species composed of six isoprene units, resulting in a total of 30 carbon atoms in their molecular structure (see **Figure 1A**). Among the various triterpenes, pentacyclic triterpenoids constitute approximately 200 different skeletons, showcasing remarkable structural diversity and potent biomedical activity[1]. Pentacyclic triterpenes that possess either five six-carbon rings (6-6-6-6-6) or four six-carbon rings and one five-carbon ring (6-6-6-6-5) are considered the most important triterpenoids [2,3].

Ursane, lupane, and oleanane types are widely distributed within higher plants, including edible plant species. Within the ursane or oleanane type, asiatic acid (AsA), ursolic acid (UrA), and oleanolic acid (OleA) represent a 6-6-6-6-6 structural arrangement. These compounds exhibit very similar structures with only small variations in the substituent groups of the rings.

Preprints (www.preprints.org) | NOT PEER-REVIEWED | Posted: 4 January 2024 doi:10.20944/preprints202401.0331.v1

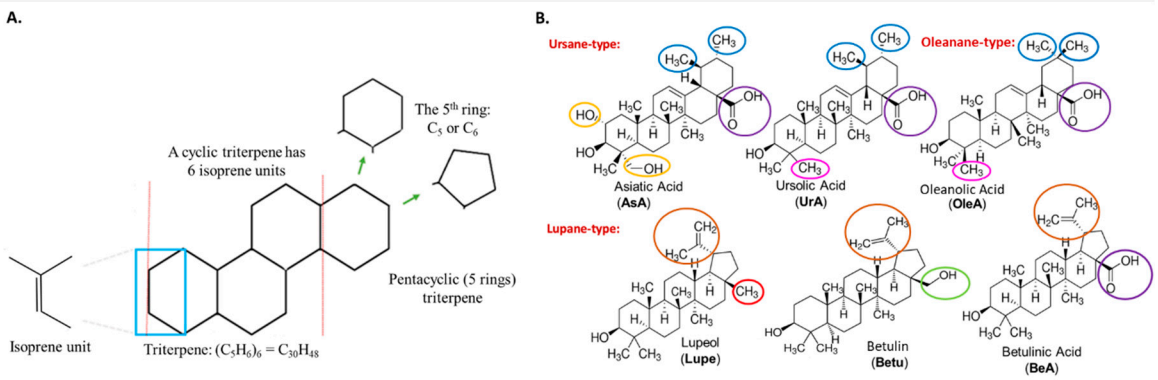

Figure 1. Structural representation of triterpenes and their substituents. **A.** Basic structure of a pentacyclic triterpene; **B.** Six pentacyclic triterpenes with their key differences highlighted in colors.

For instance, AsA possesses an additional hydroxyl group at position 2 and a hydroxymethyl substituent at position 4. On the other hand, OleA differs from UrA in that a methyl substituent has been moved from position 19 to position 20. **Figure 2.** provides a visual representation highlighting the differences between these pentacyclic triterpenes.

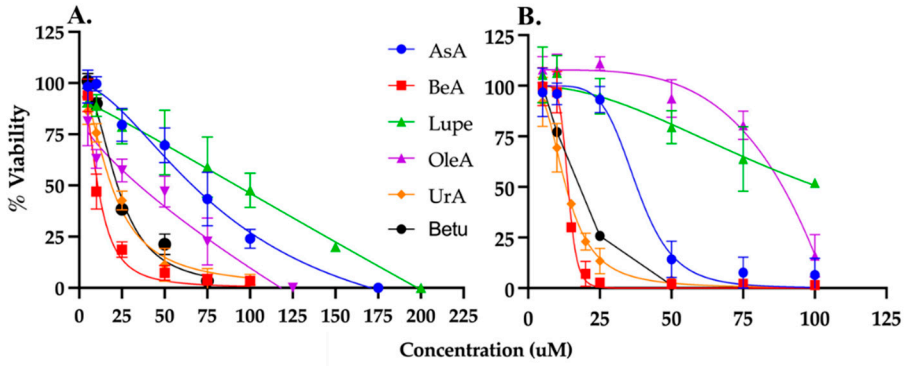

Figure 2. Viability assays. Triterpenes were incubated for 24 hours in **A.** A549 and **B.** MRC5 cells. All the triterpenes were cytotoxic to A549 and MRC5 cells at micromolar range.

Interestingly, the lupane-type pentacyclic triterpenes, namely lupeol (Lupe), betulin (Betu), and betulinic acid (BeA), exhibit a 6-6-6-6-5 structural arrangement. The primary distinction among these three compounds lies in the substituent group at position 17. Specifically, Lupe possesses a methyl group, Betu contains a hydroxymethyl group, and BeA features a carboxylic acid group at that position (**Figure 1B**). These subtle but specific variations among these six pentacyclic triterpenoids may play a crucial role in their activity across metabolic pathways, especially in cancer[4].

Cancer is a leading cause of death around the world. Lung cancer is the most common cause of cancer-related deaths. Approximately 85% of all lung cancers are non-small cell lung carcinoma (NSCLC) [5]. Unfortunately, existing therapies do not cure most NSCLC patients. Even chemotherapy (e.g., cisplatin (CisPt)), the preferred and most effective treatment for lung cancer, only shows a complete response in 30% of individuals with NSCLC [6]. Additionally, chemoresistance, which results in more aggressive cancer cells, limits the efficacy of chemotherapy. Approximately 10–15% of the patients receiving cisplatin will relapse and invariably develop chemoresistance with an expectance of no longer than a year [7]. For these reasons, new, less invasive treatments and adjuvant therapies are needed. Pentacyclic triterpenes have demonstrated great potential against NSCLC in vitro and in vivo [8] and could work to overcome drug resistance mechanisms [9].

Herein, we investigated the structure-activity-relationship against NSCLC of the six pentacyclic triterpenes AsA, UrA, OleA, Lupe, Betu, and BeA. In order to study this relationship, we determined the impact on cell cycle, DNA, mitochondrial membrane, production of reactive oxygen and nitrogen

 doi:10.20944/preprints202401.0331.v1

species (ROS/RNS), and activation of apoptosis and/or autophagy. In addition, we determined the protein expression of the mitogen-activated protein kinase/phosphatidylinositol 3-kinase (MAPK/PI3K), and gene expression of programmed death-ligand 1 (PDL1) and signal transducer and activator of transcription 3 (STAT3), key markers of chemoresistance in NSCLC. This study opens promising perspectives for further research on the role of triterpenoids as therapeutics, which ultimately will contribute to a more rational application in lung cancer therapy.

2. Materials and Methods

2.1. Chemicals and Reagents

Aqueous solutions were prepared with sterile (autoclave conditions: 121 °C and 18 PSI) high quality nanopure water (18.2 MΩ cm resistivity, Thermoscientific® Easypure water purifier).

Asiatic acid, ursolic acid, oleanolic acid, betulin, lupeol, betulinic acid were purchased from Sigma-Aldrich (St. Louis, MO, USA). The cell lines A549 (human lung adenocarcinoma; ATCC CCL-185) and MRC5 (human fibroblast-like cells; ATCC CCL-171) were from the American Type Culture Collection (Manassas, VA, USA). CellTiter 96 aqueous non-radioactive cell proliferation assay (3-(4,5-dimethylthiazol-2-yl)-5-(3-carboxymethoxyphenyl)-2-(4-sulfophenyl)-2H-tetrazolium (MTS) reagent) was from Promega Corporation (Madison, WI, USA). Cell cycle, MAPK/PI3K expression, caspase-3 activation, DNA damage, nitric oxide (NO) and oxidative stress assays were from Luminex Corporation (Austin, TX, USA). All other chemicals were purchased from various suppliers in analytical grade and used without further purification.

2.2. Cell Culture Conditions

Human NSCLC A549 and normal lung MRC5 cell lines were maintained following ATCC protocols. These cells were cultured in Dulbecco's Modified Eagle's Medium (DMEM-high glucose, containing 1% L-glutamine, 10% fetal bovine serum (FBS), and 1% penicillin/streptomycin). Cells were kept in a humidified incubator under 5% CO_2 and 95% air at 37 °C. We conducted all the experiments before the cells reached 25 passages. In all the cellular mechanistic experiments, we included CisPt as a control to compare the effects of the six pentacyclic triterpenes with the most used chemotherapy in NSCLC.

2.3. Cell Viability

The 50% inhibitory concentration (IC_{50}) of some of these triterpenes in A549 NSCLC cells were previously determined by us [10]. A similar procedure was done to determine the IC_{50} of the triterpenes in a normal lung fibroblast cell line (MRC5). In brief, MRC5 cells were seeded into 96-well plates at a density of 1×10^5 cells/mL in supplemented DMEM medium. After 24 hours, cells were treated with several concentrations (5, 10, 25, 50, 75, 100 μM) of the triterpenes (BeA, Lupe, Betu, OleA, UrA, AsA), and incubated for 24 hours. Then, 10 uL of the MTS reagent from CellTiter 96® Aqueous Non-Radioactive Cell Proliferation Assay (Promega G5421) was added to each well. Then, we incubated the plate at 37 °C and 5% CO_2 atmosphere for 1-hour. After incubation, absorbance was measured at 492 nm (n = 8) in the microplate reader spectrophotometer (Thermoscientific Multiskan FC). The cell viability was calculated as follows:

% Viability = (sample data − incubation media data) / (untreated cells data − incubation media data) × 100

Cell viability data is presented as mean ± SD of at least three independent experiments. IC_{50} values were calculated with the GraphPad Prism 9 software (Prism 9; GraphPad by Dotmatics, San Diego, CA, USA) using the dose-response curve. The data were normalized by the non-linear fit of log (drug inhibition) vs. normalized response-variable slope to obtain the best fit IC_{50} and R-squared values.

 doi:10.20944/preprints202401.0331.v1

2.4. Flow Cytometry Analysis

We used flow cytometry to analyze several cellular mechanistic pathways in A549 cells after incubation with the triterpenes. In general, cells were seeded in a 6-well plate at a density of 1×10^6 cells/mL and incubated for 24 hours in supplemented DMEM. After 24 hours, A549 cells were treated with triterpenes, followed by each manufacturer protocol. All these following experiments were performed in a Muse Cell Analyzer (Muse® Cell Analyzer; EMD Millipore Corporation, Temecula, CA, USA). The concentration of the triterpenes in each assay was selected depending on the cellular concentration necessary to generate the signal in the instrument.

2.4.1. Cell Cycle Arrest

A549 cells were incubated with triterpenes (IC_{35}) for 24 hours. Then, cells were scraped, centrifuged, and then fixed using cold 70% ethanol. Afterward, the fixed cell pellet was incubated with the cell cycle reagent (Luminex MCH100106 kit) for 30 min for immediate measurement.

2.4.2. DNA Damage Induction

A549 cells were incubated with triterpenes (IC_{50}) for 24 hours. Then, A549 cells were scraped and centrifuged. The pellet was suspended in the assay buffer from the Luminex MCH200107 kit. Later, the cell pellet was fixed and permeabilized. Afterward, the antibody cocktail was added and incubated for 30 min. Next, the cell pellet was washed and suspended in fresh assay buffer for measuring.2.4.3 Mitochondrial Polarization

Muse™ MitoPotential Kit (Luminex MCH100110) was used to determine mitochondrial polarization. After the treatment incubation with triterpenes (IC_{35}) for 24 hours, Muse™ MitoPotential working was added and incubated for 20 min at 37°C. Next, MuseTM 7-AAD was added and incubated for 5 minutes at room temperature. Finally, a brief mix was given to each sample before measuring.

2.4.4. Caspase 3 Activation

A549 cells were incubated with triterpenes (IC_{50}) for 24 hours. A549 cells were scraped and centrifuged. The pellet was dissolved in the assay buffer provided by Luminex MCH100108 kit. Then, the fluorescently labeled caspase-3 substrate was added to the dissolved pellet and incubated for 30 min at 37 °C in a 5% CO_2 atmosphere for immediate measurement.

2.4.5. Oxidative Stress

Production of reactive oxygen species (ROS) and reactive nitrogen species (RNS) was determined using the Oxidative Stress kit (Luminex MCH100111) and Nitric Oxide kit (MCH100112). After A549 cells were treated with triterpenes (IC_{50}) for 24 hours, the cells were scraped and centrifuged. For ROS, cell pellet was incubated with DHE dye for 1-hour at 37°C. For RNS, cell pellet was incubated with DAX-J2 Orange dye for 30 min at 37°C.

2.4.6. Autophagy activation

Muse® Autophagy LC3-antibody Based Kit (Luminex MCH200109) was used to determine autophagy activation. After A549 cells were treated with triterpenes (IC_{35}) for 24 hours, autophagy reagent A was added for 2~6 hours. Then the cells were detached and centrifuged. The pellet was suspended and incubated for 30 minutes in the autophagy reagent B containing anti-LC3 mouse monoclonal antibody. Finally, the cell pellet was washed and suspended in fresh assay buffer for measuring.

2.4.7. MAPK/PI3K Expression

Muse® P13K/MAPK Dual Pathway Activation Kit (Luminex MCH200108) was used to determine MAPK/PI3K expression. After the treatment incubation with triterpenes (IC_{35}) for 24 hours,

 doi:10.20944/preprints202401.0331.v1

A549 cells were scraped, centrifuged, and washed once with 1X PBS. Next, the fixation buffer was incubated for 10 min and then the permeabilization buffer for another 10 min. Both incubations were on ice. Later, the antibody cocktail containing Anti-phospho-Akt and Anti-phospho-ERK1/2 was incubated for 30 min. Afterward, the cell pellet was washed and suspended in fresh assay buffer for measuring.

2.5. RNA extraction and quantitative real-time PCR

A549 cells were seeded into 6-well plates at a density of 1×10^6 cells/mL in supplemented DMEM. Cells were incubated with triterpenes (IC_{35}) for 24 hours. Total RNA was extracted from the cells using TRIzol reagent (Invitrogen) according to the manufacturer's instructions. The purity and concentration of RNA were assessed using a NanoDrop spectrophotometer (ThermoScientific). cDNA was synthesized using the High-Capacity cDNA Reverse Transcription Kit (Applied Biosystems) according to the manufacturer's instructions.

Real-time qPCR was performed on a StepOnePlus Real-Time PCR System (Thermo Fisher Scientific) using TaqMan Gene Expression Assays for PDL1 (CD274; Assay ID: Hs01125297_m1), and STAT3 (Assay ID: Hs01047586_g1). Each reaction consisted of 10 ng of cDNA, TaqMan Gene Expression Master Mix (Applied Biosystems), and TaqMan probes. The PCR cycling conditions were as follows: 95°C for 10 min, followed by 40 cycles of 95°C for 15 s and 60°C for 60 s. The relative gene expression levels were calculated using the ΔΔCt method. GAPDH (Assay ID: Hs02758991_g1) was used as the endogenous control for normalization.

2.6. Statistical Analysis

All experiments were performed at least in triplicate. All data were expressed by plotting values with an average of four to eight measurements for each treatment condition as mean ± SD and analyzed with the software GraphPad Prism 9 (San Diego, CA, USA). Statistical analysis was performed using one-way analysis of variance (ANOVA) to compare the mean value of each treated cells versus the control (untreated cells). The statistical significance defined by the software for P values are: **** < 0.0001, *** from 0.001 to 0.0001, ** from 0.001 to 0.01, * from 0.01 to 0.05, and non-significant (n.s.) ≥ 0.05.

3. Results

3.1. Viability and IC_{50} in NSCLC and lung fibroblast cells

MTS/PMS colorimetric assay was used to determine the viability of cells exposed to the triterpenes generating a dose-response curve for NSCLC A549 cells and normal lung fibroblast MRC5 cells. Each triterpene was incubated at several μM concentrations for 24hours to determine the IC_{50}. As expected, cell viability decreases at increasing drug concentration (**Figure 2**). The IC_{50} values were calculated using the data from **Figure 2** and summarized in **Table 1**. UrA was the most cytotoxic triterpene in MRC5 cells, and BeA was the most cytotoxic in the A549 cell line. In contrast, Lupe was the least cytotoxic in both cell lines.

The therapeutic index (TI) is a measurement of selectivity comparing the IC_{50} of a drug against non-cancerous vs cancerous cells. The OleA showed the highest TI (= 2), while UrA showed the lowest TI (= 0.57). Interestingly, Lupe and BeA have the same TI but BeA with the lowest IC_{50} for both cell lines.

Table 1. A549 and MRC5 IC_{50} and TI for each pentacyclic triterpene under study.

Triterpenes	A549 IC_{50} (μM)	MRC5 IC_{50} (μM)	TI[#]
AsA	59 ± 6*	38 ± 2	0.64
OleA	43 ± 5*	86 ± 2	2.00
UrA	23 ± 1*	13 ± 1	0.57
BeA	15 ± 0.7*	19 ± 0.4	1.27

Preprints (www.preprints.org) | NOT PEER-REVIEWED | Posted: 4 January 2024 doi:10.20944/preprints202401.0331.v1

Lupe	80 ± 6*	101 ± 8	1.26
Betu	22 ± 1	16 ± 0.5	0.73

*These results were previously published by us [10]. #TI = MRC5 IC_{50} / A549 IC_{50}, where >1 means higher selectivi.ty

3.2. Cell cycle arrest and DNA damage

Following a 24-hour treatment period, **Figure 3A** demonstrates that all pentacyclic triterpenes produced cell cycle arrest in A549 cells at the S-phase and G2/M phase in comparison to the negative control (untreated cells) and greater cycle arrest in G2/M in comparison to CisPt.

In contrast, only UrA and AsA caused activation of the DNA damage machinery compared to the negative control (untreated cells), as shown in **Figure 3B.** UrA demonstrated to induce a similar DNA damage extent as the CisPt chemotherapy.

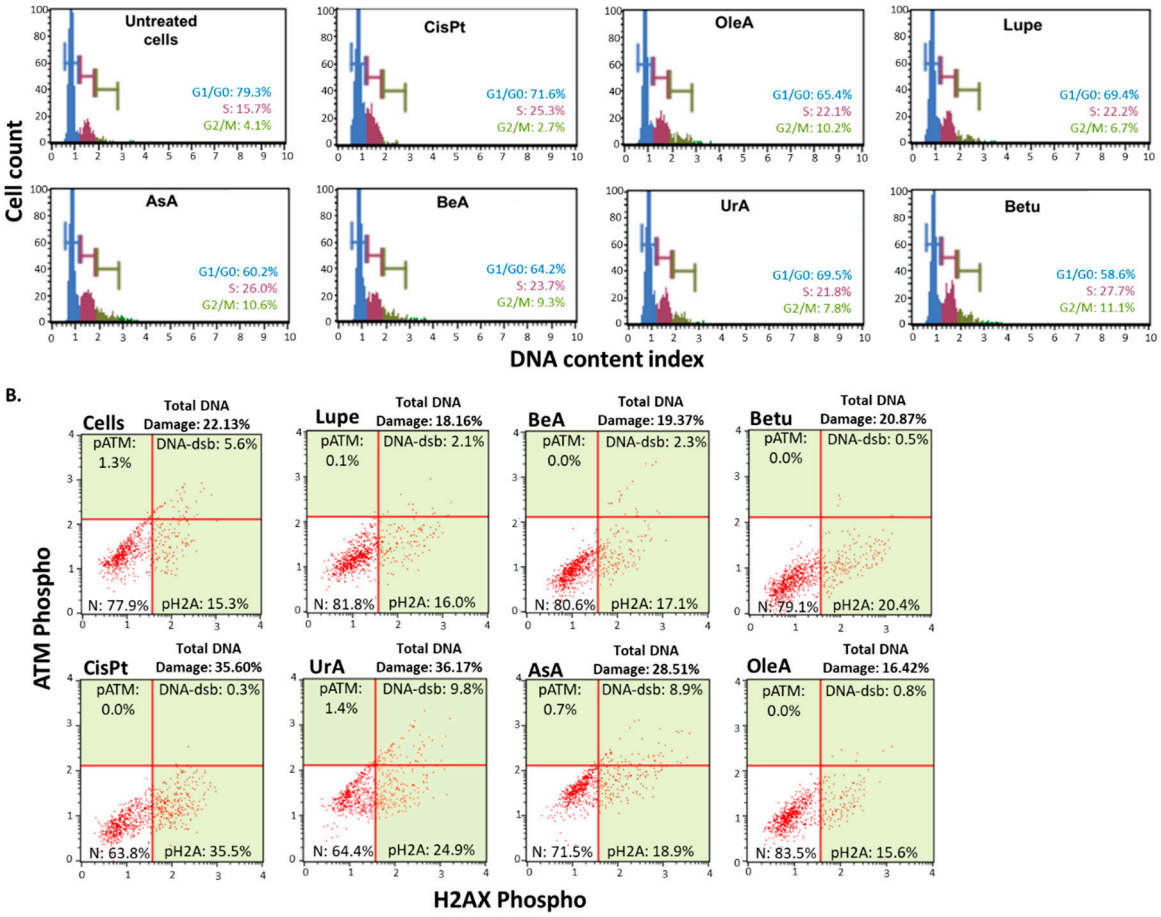

Figure 3. Nuclear-related pathways. A. Cell cycle arrest assay. All the pentacyclic triterpenes induced cell cycle arrest at the S-phase and G2/M; **B.** DNA damage assay. Only UrA and AsA induced activation of the DNA damage machinery.

3.3. Mitochondrial membrane permeability and Caspase-3 activity

Figure 4A shows that following a 24-hour treatment period, Betu was the only pentacyclic triterpene that induced only a slight depolarization of the mitochondria when compared to the negative control (untreated cells).

Figure 4B shows that all triterpenes activated caspase 3 enzymatic machinery during a 24-hour treatment period, except for Lupe compared to the negative control (untreated cells). However, UrA, Betu and OleA produced higher caspase 3 activation than CisPt, where UrA was the highest.

Preprints (www.preprints.org) | NOT PEER-REVIEWED | Posted: 4 January 2024 doi:10.20944/preprints202401.0331.v1

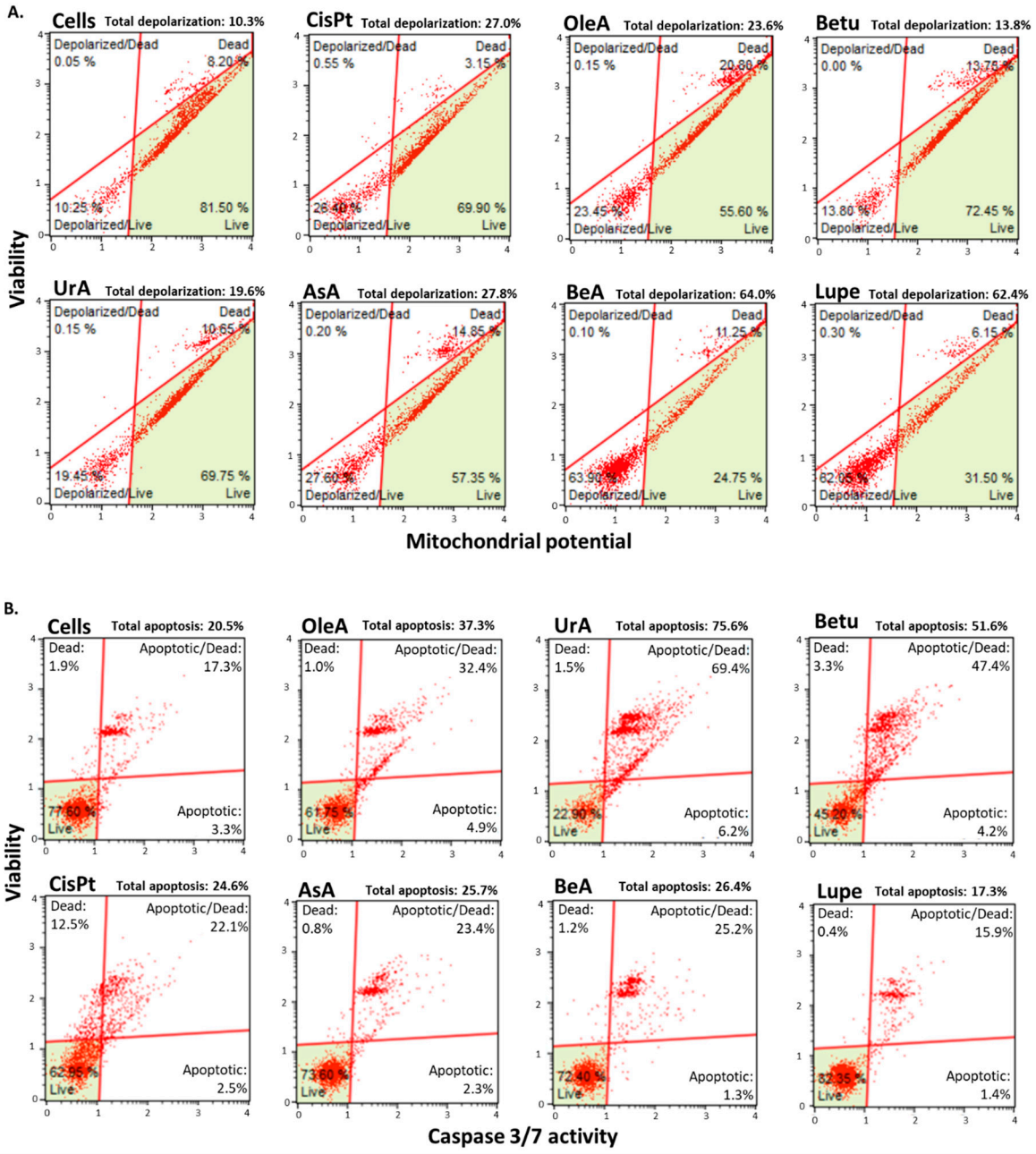

Figure 4. Mitochondrial-related pathways. A. Mitochondrial membrane permeability assay. All the pentacyclic triterpenes induced depolarization of the mitochondria except Betu. BeA and Lupe showed the strongest depolarization effect; **B.** Caspase-3 activity assay. All the triterpenes activated caspase-3 except Lupe. UrA, Betu, and OleA showed the highest activation.

3.4. Autophagy, reactive nitrogen species (RNS), and mitochondrial ROS production (mROS)

Figure 5A shows that after 24 hours of incubation, only UrA, AsA, and Betu induce the production of RNS compared to the controls. Betu was the triterpene that induced the highest RNS production. In contrast, OleA, Lupe and BeA did not induce RNS, similar to CisPt.

Figure 5B shows that all triterpenes increased the superoxide ROS generated from mitochondria after 24 hours compared with the negative control, and some of them higher than CisPt. BeA caused the largest level of ROS, whereas the lowest was by AsA.

Figure 5C shows that Betu, AsA, and UrA induced autophagic response similar to CisPt, and comparing to the controls (negative control untreated cells ratio = 0.8 and positive control untreated

Preprints (www.preprints.org) | NOT PEER-REVIEWED | Posted: 4 January 2024 doi:10.20944/preprints202401.0331.v1

starving cells ratio = 1). BeA has a similar ratio to the untreated cells, while Lupe and OleA showed to inhibit the LC3 activity.

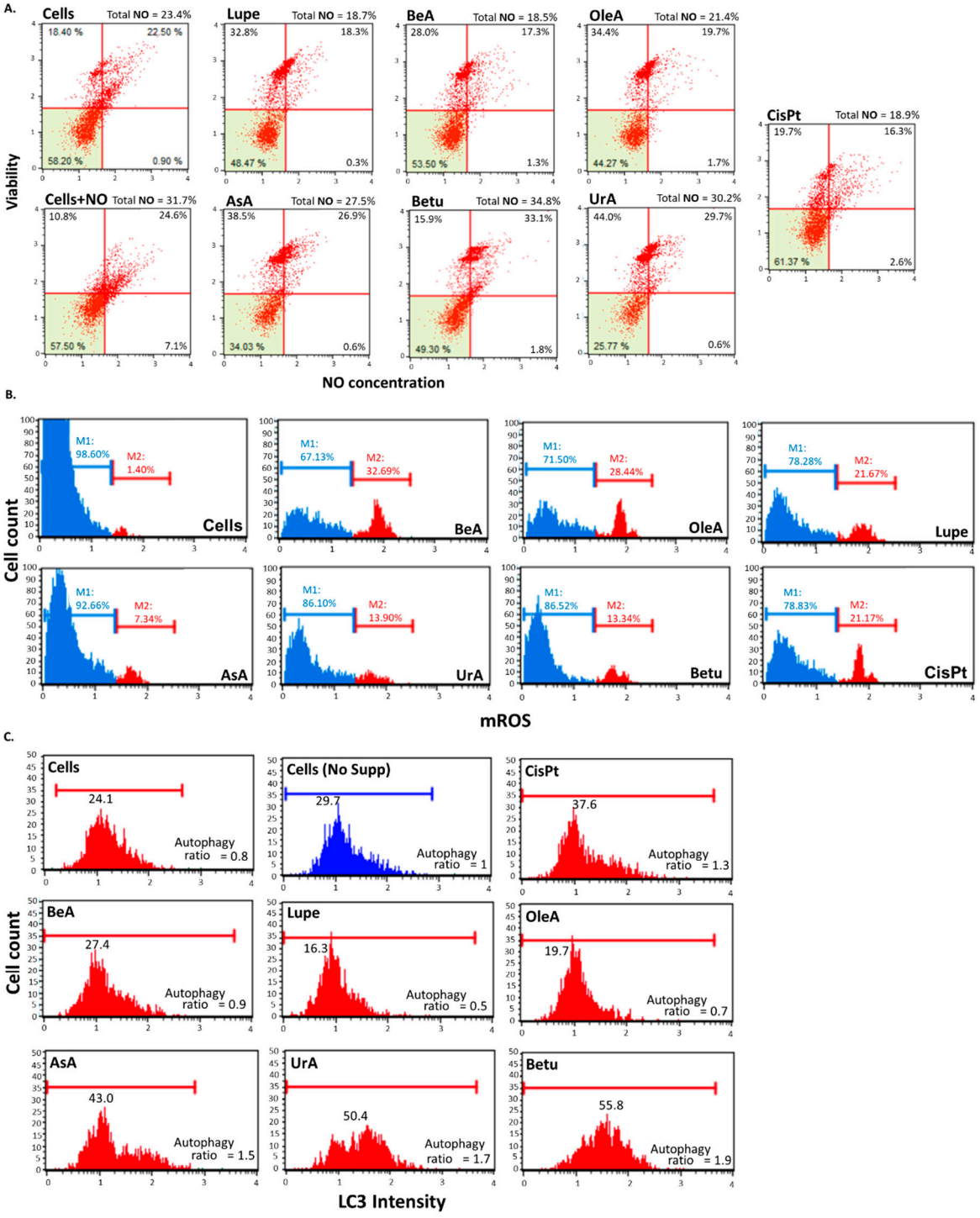

Figure 5. Oxidative stress-related processes. A. RNS Assay. For this experiment, we included a positive control by only adding NO to the cells. Only UrA, AsA and Betu produced NO. **B.** Mitochondrial ROS production assay. DHE (Dihydroethidium) dye reacts with the superoxide species mostly produced by mitochondrial damage. All the six triterpenes induced the production of ROS. **C.** Autophagy induction assay. For this experiment, we included a positive control by removing the serum from the culturing medium (starvation) of the untreated cells. Betu, AsA and UrA activated autophagic response.

Preprints (www.preprints.org) | NOT PEER-REVIEWED | Posted: 4 January 2024 doi:10.20944/preprints202401.0331.v1

3.5. MAPK/PI3K protein expression and PDL1 and STAT3 gene expression

Figure 6A shows that UrA is the only one that induces simultaneous expression of MAPK and PI3K similar to CisPt, while Betu and BeA could slightly inhibit the total expression of MAPK/PI3K, compared to untreated cells. In contrast, AsA, Lupe and OleA did not affect the expression of MAPK/PI3K.

In the RT-qPCR gene expression assays (**Figure 6B**), most of the triterpenes significantly inhibited both PDL1 and STAT3. OleA and Betu on the other hand, did not inhibit the STAT3 and PDL1 genes, respectively. The lupane-type BeA is better at suppressing both genes.

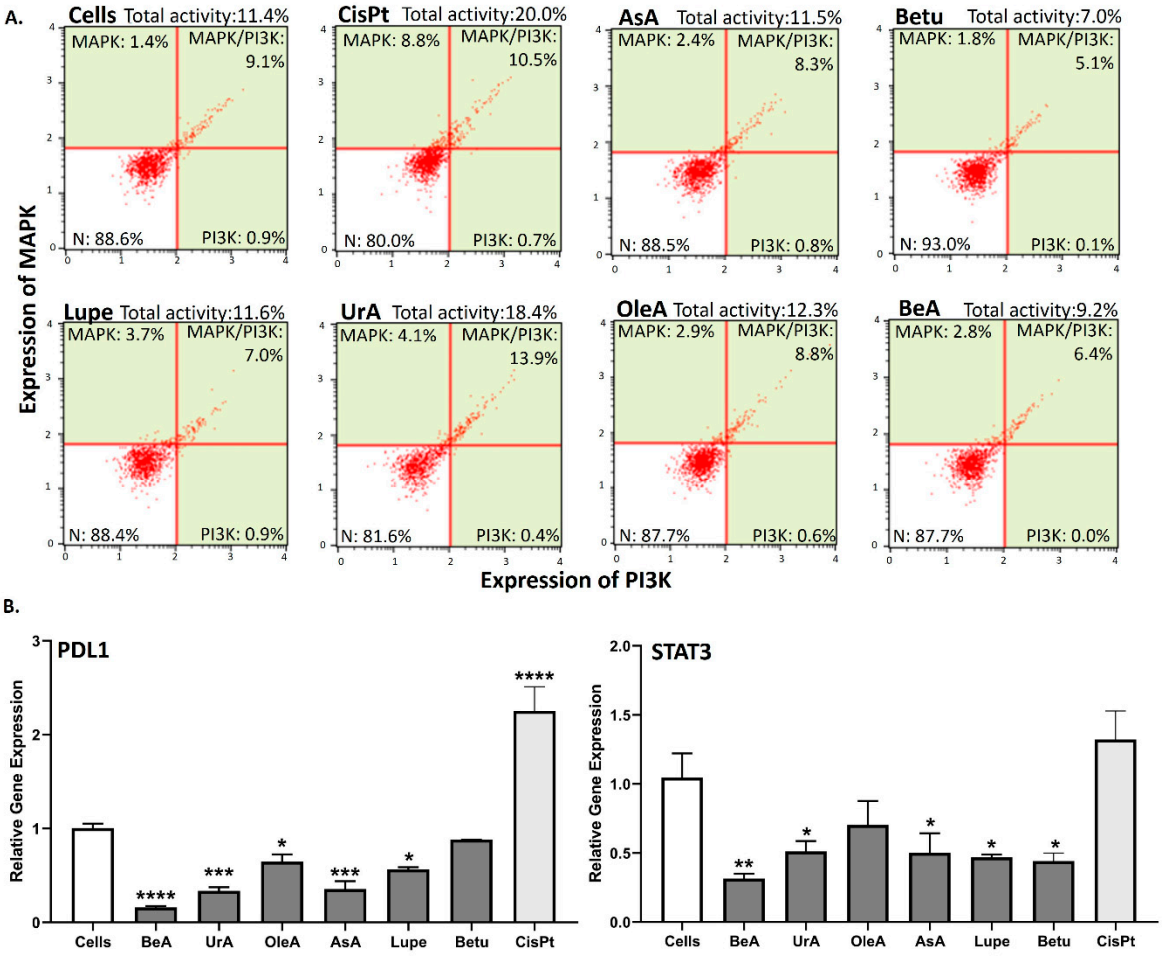

Figure 6. Protein and gene expression assays. A. MAPK/PI3K protein expression. Only UrA increased the MAPK/PI3K expression. **B.** PDL1 and STAT3 gene expression using real-time qPCR. Only OleA and Betu did not inhibit the STAT3 and PDL1 genes, respectively.

3.7. Results Summary

Table 2 provides a summary of the findings from all the mechanistic pathways studied in this project. The lupane-type BeA is the pentacyclic triterpene that affect most of the key pathways with less concentration (lowest IC_{50}), and is the most potent in mitochondrial depolarization, production of mROS and downregulation of STAT3 and PDL1 in the NSCLC A549 cells. These results indicate that the structure of the triterpenes affect the interaction with different pathways.

Preprints (www.preprints.org) | NOT PEER-REVIEWED | Posted: 4 January 2024 doi:10.20944/preprints202401.0331.v1

Table 2. Summary of the mechanistic pathways results

Mechanism	UrA	AsA	OleA	Lupe	BeA	Betu	Highest	Lowest
TI > 1	-	-	✓	✓	✓	-	OleA	UrA
Cell cycle arrest	✓	✓	✓	✓	✓	✓	Betu	UrA
DNA damage	✓	✓	-	-	-	-	UrA	OleA
Mitochondrion depolarization	✓	✓	✓	✓	✓	-	BeA	Betu
Caspase 3 activation	✓	✓	✓	-	✓	✓	UrA	Lupe
RNS production	✓	✓	-	-	-	✓	Betu	BeA
mROS production	✓	✓	✓	✓	✓	✓	BeA	Betu
Autophagy inhibition	-	-	✓	✓	✓	-	Lupe	Betu
MAPK/PI3K inhibition	-	✓	✓	✓	✓	✓	Betu	UrA
PDL1 downregulation	✓	✓	✓	✓	✓	-	BeA	Betu
STAT3 downregulation	✓	✓	-	✓	✓	✓	BeA	OleA

4. Discussion

Triterpenes are known for their wide range of benefits, including their anti-inflammatory, antimicrobial, antiviral, analgesic, anti-tumorigenic, and immunomodulatory characteristics [11]. Our investigation sought to unravel the interplay between structural variations governing the bioactivity of six lupane, oleanane, and ursane-type pentacyclic triterpenes and their impact on NSCLC cells. This study dive into the underlying mechanistic principles with a particular emphasis on key pathways to induce cells death (i.e., cell cycle arrest, DNA damage, permeability of mitochondrial membrane, activation of caspase 3, and oxidative stress) but also in chemoresistance-related processes (i.e., inhibition of autophagy, MAPK/PI3K, STAT3 and PDL1 expression).

Our experimental results revealed distinct patterns in the response of NSCLC cells to the six pentacyclic triterpenes under scrutiny. In the viability assays, results demonstrated that Lupe has the highest IC_{50}, OleA the best TI, and BeA has the lowest IC_{50} with a TI >1. Normal lung cells such as MRC5 have been considered as cancer associated fibroblasts (CAF) even when they are non-cancerous cells [12]. This means that an effective therapy must kill both cell lines (NSCLC and CAF) but aggressively to cancerous cells. In this way, BeA showed the lowest IC_{50} to kill both cell lines (NSCLC and CAF) but more aggressively to the NSCLC A549 of the six triterpenes. These results suggested that a methyl substituent in lupane-type triterpenes instead of carboxylic acid or hydroxyl can drastically diminish its cytotoxicity. On the other hand, changes in the methyl substituents in OleA (vs UrA) diminished their cytotoxicity in cells but increased the selectivity. Previous studies have found similar IC_{50} in the μM range in a 24-hour treatment period for the six selected pentacyclic triterpenes exposed to different cancer cell types [13–18]. This highlights the versatility of the use of triterpenes against cancer in different organs and tissues.

Nuclear processes as the cell cycle are important pathways to promote cancer progression. Cell cycle arrest in response to DNA damage is a critical mechanism that helps prevent the propagation of cancer cells and to induce apoptosis [19]. In this study, all triterpenes produced cell cycle arrest in S-phase and G2/M phase. There are several studies that showed similar results where these triterpenes exhibited S-phase and G2/M phase arrest in myeloma, gastric, breast and lung cancer cells. [20–24]. These results suggest that regardless of structural variations, these six pentacyclic triterpenes may trigger cell cycle arrest in these two critical divisions in NSCLC, implying they all may be able to prevent the proliferation of these cancer cells. In addition, only the ursane-type, UrA, and AsA caused DNA damage, implying their other potential targets to kill cancer cells compared to the other four triterpenes. These results revealed that, unlike lupane-type, ursane-type triterpenes might employ DNA damage machinery to induce apoptosis. These results support previous studies that highlight UrA to increase DNA damage and chemosensitizing A549 cells [25]. In contrast, there are several studies that demonstrated that lupane-type triterpenes are able to cause DNA damage [26,27].

 doi:10.20944/preprints202401.0331.v1

Another important pathway is the activation of apoptosis through the mitochondrial response. Disruption of the mitochondrial membrane potential can lead to the release of cytochrome c, which activates caspase 3, initiating apoptosis and then, cell death [28]. From our results, all the triterpenes induced depolarization of the mitochondrion except Beu. Our findings suggested that a lupane-type triterpene (6-6-6-6-5 ring structure) with a methyl (Lupe) or a carboxylic acid (BeA) substituent can induce high mitochondrial membrane permeability (even higher than CisPt). On the other hand, the ursane-type (UrA and AsA) and OleA, each with a 6-6-6-6-6 ring structural arrangement but varying substituents, induced a mild membrane depolarization.. Most of the studies in the literature showed that pentacyclic triterpenes permeabilize mitochondrion [23,27,29]. Furthermore, all the triterpenes except Lupe activated caspase 3. Interestingly, the triterpenes that less affect the mitochondrial potential greatly increase the caspase activity (and vice versa). This outcome could mean that a greater effect to the mitochondrial potential could cause the inactivation of the complexes in the electron transport chain, e.g., cytochrome c. Another explanation that supports our argument is that membrane depolarization is not a requirement to release cytochrome c from mitochondrion [30,31]. The proapoptotic protein Bid can translocate the mitochondrion to induce the release of cytochrome c and caspase-8 can directly activate caspases 3/7 [32]. This explains why Betu slightly affects the membrane potential but activated a relatively high amount of caspase 3 compared to the other triterpenes. This suggests that caspase-3 activation in Betu-induced apoptosis may not be solely on mitochondrial membrane permeability.

Oxidative stress such as RNS and ROS levels can modulate autophagy. Mild amounts of ROS and RNS promote the autophagic response, while high concentrations inhibit autophagy and promote cell death [33,34]. Although all triterpenes produced ROS, comparing to untreated cells, the amount of ROS from BeA, OleA and Lupe are an average of 26.2%, while Betu, AsA and UrA are an average of 10.1%. Thus, BeA, OleA, and Lupe did not activate autophagy because of the high concentration of ROS. On the other hand, Betu, AsA and UrA activated the autophagic response by the lower levels of ROS. In the case of RNS, the triterpenes that increased the concentration of RNS are Betu, AsA and UrA. However, compared to untreated cells, the production of RNS for these triterpenes is mild (an average of 7.4%). For this reason, the levels of RNS did not influence the activity of LC3. Based on the structural side of these triterpenes, our results suggested that the skeletal carbon rings structure of the pentacyclic triterpenes is essential in triggering the formation of mitochondrial-derived ROS. Also, they revealed that most of the difference in the six pentacyclic triterpenes structures and their substituents did not inhibit ROS production. A possible explanation is that these triterpenes inhibit complex I or complex III in the electron transport chain. Moreover, the results from the mROS assay correspond with the results from the mitochondrial potential assay, where BeA has the greater induction of RNS and mROS and Betu the lowest. In the case of RNS, our findings suggested that the ursane-type pentacyclic triterpenes are more important in RNS production than lupane-type and oleanane-type. The change in the positions of the methyl groups at the 5th ring in OleA compared with the ursane-type triterpenes completely abrogated the RNS production. Regarding lupane-type triterpenes, a change of the carboxylic or methyl group for a hydroxyl, such as Betu, drastically improves its effects in RNS production. Numerous studies agreed with our results that triterpenes can induce cell death by the production of ROS, as summarized in the following review [35]. In contrast, we found few studies of the effect of triterpenes in the production of RNS, where they found the inhibition of NO by BeA and OleA, and the production of NO by UrA [36,37] similar to our results. In the case of autophagic response, results in the literature are contradictory. BeA has demonstrated different results depending on the cell type and concentration [38,39]. In the same study UrA demonstrated to increase the production of NO, they found to induce autophagy [37]. In is important to understand that autophagy can suppress tumor development in the early stages, but once the tumor is established, promotes chemotherapy resistance [40].

MAPK/PI3K has been linked to the upregulation of PDL1, which leads to immune suppression and chemoresistance [41]. Meanwhile, STAT3-mediated upregulation of PDL1 expression on cancer cells [41]. In our experiments, only UrA slightly increased the expression of MAPK/PI3K when

compared to negative (untreated cells) and positive (CisPt) controls. These results suggested that lupane-type triterpenes with a 6-6-6-6-5 structural arrangement are better in limiting cell progression and survival by MAPK/PI3K independently of the substituents. Regarding the chemoresistance-markers, STAT3 and PDL1, our results revealed that most of the pentacyclic triterpenes suppress these two genes where the chemotherapy CisPt clearly upregulated PDL1. However, BeA was the greater inhibitor of the MAPK/PI3K expression, and PDL1 and STAT3 gene expression in A549. In the literature, we found similar results for MAPK, PI3K, PDL1 and STAT3 after BeA treatment [42,43]. UrA also showed to downregulate STAT3 and PDL1 [44].

In summary, BeA emerge as the triterpenes exerting the most widespread influence on several key pathways to induce mitochondrial-based apoptosis with the lowest IC_{50}, a TI > 1 and inhibit the chemoresistance-related genes STAT3 and PDL1. Furthermore, we previously demonstrated that BeA synergizes with doxorubicin to increase the effectivity of this drug in A549 cells [45]. These findings collectively indicate that triterpenes impact different pathways depending on the substituents of their rings. This study strongly supports using pentacyclic triterpenoids in NSCLC and emphasize BeA as the best possible alternative.

5. Conclusions

This study significantly advances our knowledge of the potential therapeutic applications of pentacyclic triterpenoids against cancer. Understanding the structure-activity relationship of these triterpenes carries profound implications for the development of targeted therapeutics. The delineation of specific structural motifs associated with enhanced anti-cancer activity provides a rational basis for the design and optimization of triterpene derivatives with improved efficacy and reduced off-target effects. For example, BeA structure can be used as the base for the synthesis of new lung cancer therapies where substituents can be added or removed to enhance its activity. In the same way, OleA can be studied to understand the structural selectivity component. This knowledge is pivotal in guiding future efforts toward the development of novel pharmaceutical interventions for lung adenocarcinoma. However, further clinical studies are warranted to explore the full potential of pentacyclic triterpenes as promising candidates for cancer treatment and their potential integration into conventional therapies to combat cancer more effectively.

Author Contributions: Conceptualization, Y.D.; formal analysis, A.T., C.G., D.P., G.T. S.E., E.V., M.M., and Y.D.; funding acquisition, Y.D.; investigation, Y.D.; methodology, A.T., D.P., G.T. S.E., M.M, E.V., V.M., and Y.D.; project administration, Y.D.; resources, Y.D.; supervision, Y.D.; validation, Y.D.; visualization, Y.D.; writing—original draft, C.G., and Y.D.; writing—review and editing, A.T., and Y.D. All authors have read and agreed to the published version of the manuscript.

Funding: This project was supported by The Sloan Scholars Mentoring Network Seed Grant and Fundación Intellectus.

Institutional Review Board Statement: Not applicable

Informed Consent Statement: Not applicable.

Data Availability Statement: Data is available upon reasonable request.

Acknowledgments: The authors would like to thank Dr. Estela Estapé (Director of the SJBSM Research Center) for her outstanding dedication and service as a senior advisor in the writing process of this paper. We also thank San Juan Bautista School of Medicine for supporting this publication.

Conflicts of Interest: The authors declare no conflict of interest. The funders had no role in the design of the study; in the collection, analyses, or interpretation of data; in the writing of the manuscript; or in the decision to publish the results.

References

1. Xu, R.; Fazio, G.C.; Matsuda, S.P.T. On the origins of triterpenoid skeletal diversity. *Phytochem* **2004**, *65*, 261–291. doi:10.1016/j.phytochem.2003.11.014.
2. Ren, Y.; Kinghorn, A.D. Natural product triterpenoids and their semi-synthetic derivatives with potential anticancer activity. *Planta Med* **2019**, *85*, 802-814. doi:10.1055/a-0832-2383.
3. Mandal, A.; Ghosh, S.; Bothra, A.K.; Nanda, A.K.; Ghosh, P. Synthesis of friedelan triterpenoid analogs with DNA topoisomerase II*α* inhibitory activity and their molecular docking studies. *Eur J Med Chem* **2012**, *54*, 137–143. doi:10.1016/J.EJMECH.2012.04.037.
4. Vo, N.N.Q.; Nomura, Y.; Muranaka, T.; Fukushima, E.O. Structure-activity relationships of pentacyclic triterpenoids as inhibitors of cyclooxygenase and lipoxygenase enzymes. *J Nat Prod* **2019**, *82*, 3311–3320. doi:10.1021/acs.jnatprod.9b00538.
5. Sung, H.; Ferlay, J.; Siegel, R.L.; Laversanne, M.; Soerjomataram, I.; Jemal, A.; Bray, F. Global cancer statistics 2020: GLOBOCAN estimates of incidence and mortality worldwide for 36 cancers in 185 countries. *CA Cancer J Clin* **2021**, *71*, 209–249. doi:10.3322/CAAC.21660.
6. Baxevanos, P.; Mountzios, G. Novel chemotherapy regimens for advanced lung cancer: Have we reached a plateau? *J Transl Med* **2018**, *6*, 139. doi: 10.21037/atm.2018.04.04.
7. Ranasinghe, R.; Mathai, M.L.; Zulli, A. Cisplatin for cancer therapy and overcoming chemoresistance. *Heliyon* **2022**, *8*, e10608. doi:10.1016/j.heliyon.2022.e10608.
8. Ghante, M.H.; Jamkhande, P.G. Role of pentacyclic triterpenoids in chemoprevention and anti-cancer treatment: An overview on targets and underling mechanisms. *J Pharmacopuncture* **2019**, *22*, 55. doi:10.3831/KPI.201.22.007.
9. Cheng, J.; Li, X.; Wang, S.; Han, Y.; Zhao, H.; Yang, X. Carrier-free triterpene prodrugs with glutathione response and biosafety for synergistically enhanced photochemotherapy. *ACS Appl Mater Interfaces* **2021**, *13*, 245–256. doi:10.1021/ACSAMI.0C19214.
10. Delgado, Y.; Torres, A.; Milian, M. Data on cytotoxic pattern of cholesterol analogs for lung adenocarcinoma cells. *Data Brief* **2019**, *25*, 104179. doi:10.1016/J.DIB.2019.104179.
11. Rufino-Palomares, E.E.; Pérez-Jiménez, A.; García-Salguero, L.; Mokhtari, K.; Reyes-Zurita, F.J.; Peragón-Sánchez, J.; Lupiáñez, J.A. Nutraceutical role of polyphenols and triterpenes present in the extracts of fruits and leaves of *Olea europaea* as antioxidants, anti-infectives and anti-cancer agents on healthy growth. *Molecules* **2022**, *27*, 2341. https://doi.org/10.3390/molecules27072341
12. Ding, S.M.; Lu, A.L.; Zhang, W.; Zhou, L.; Xie, H.Y.; Zheng, S.S; Li, Q.Y. The role of cancer-associated fibroblast MRC-5 in pancreatic cancer. *J Cancer* **2018**, *9*, 614-628. doi:10.7150/jca.19614.
13. Guo, W.; Xu, B.; Wang, X.; Zheng, B.; Du, J.; Liu, S. The analysis of the anti-tumor mechanism of ursolic acid using connectively map approach in breast cancer cells line MCF-7. *Cancer Manag Res*. **2020**, *12*, 3469-3476. doi:10.2147/CMAR.S241957.
14. Wróblewska-Łuczka, P.; Cabaj, J.; Bąk, W.; Bargieł, J.; Grabarska, A.; Góralczyk, A., Łuszczki, J. J. Additive interactions between betulinic acid and two taxanes in in vitro tests against four human malignant melanoma cell lines. *Int J Mol Sci* **2022**, *23*, 9641. doi:10.3390/ijms23179641.
15. Pantia, S.; Kangsamaksin, T.; Janvilisri, T.; Komyod, W. Asiatic acid inhibits nasopharyngeal carcinoma cell viability and migration via suppressing STAT3 and Claudin-1. *Pharmaceuticals* **2023**, *16*, 902. doi:10.3390/ph16060902.
16. Gao, C.; Li, X.; Yu, S.; Liang, L. Inhibition of cancer cell growth by oleanolic acid in multidrug resistant liver carcinoma is mediated via suppression of cancer cell migration and invasion, mitochondrial apoptosis, G2/M cell cycle arrest and deactivation of JNK/p38 signalling pathway. *J BUON* **2019**, *24*, 1964-1969.
17. Król, S. K.; Kiełbus, M.; Rivero-Müller, A.; Stepulak, A. Comprehensive review on betulin as a potent anticancer agent. *Biomed Res Int* **2015**, *2015*, 584189. doi:10.1155/2015/584189.
18. Pitchai, D.; Roy, A.; Ignatius, C. In vitro evaluation of anti-cancer potentials of lupeol isolated from Elephantopus scaber L. on MCF-7 cell line. *J Adv Pharm Technol Res* **2014**, *5*, 179-184. doi:10.4103/2231-4040.143037.
19. Ford, J.M.; Kastan, M.B. 10 - DNA Damage Response Pathways and Cancer. In *Abeloff's Clinical Oncology (Fifth Edition)*, Niederhuber, J.E., Armitage, J.O., Doroshow, J.H., Kastan, M.B., Tepper, J.E., Eds.; Churchill Livingstone: Philadelphia, 2014; pp. 142-153.e143.
20. Aborehab, N.M.; Salama, M.M.; Ezzat, S.M. A novel lupene derivative from Thymus capitatus possesses an apoptosis-inducing effect via Let-7 miRNA/Cyclin D1/VEGF cascade in the A549 cell line. *BMC Complement Med Ther* **2023**, *23*, 365. doi:10.1186/s12906-023-04201-7.
21. Zhan, X.K.; Li, J.L.; Zhang, S.; Xing, P.Y.; Xia, M.F. Betulinic acid exerts potent antitumor effects on paclitaxel-resistant human lung carcinoma cells (H460) via G2/M phase cell cycle arrest and induction of mitochondrial apoptosis. *Oncol Lett* **2018**, *16*, 3628–3634.

22. Shen, M.; Hu, Y.; Yang, Y.; Wang, L.; Yang, X.; Wang, B.; Huang, M. Betulinic acid induces ROS-dependent apoptosis and S-phase arrest by inhibiting the NF-kappaB pathway in human multiple myeloma. *Oxid Med Cell Longev* **2019**, *2019*, 5083158.
23. Weng, H.; Tan, Z.-J.; Hu, Y.-P.; Shu, Y.-J.; Bao, R.-F.; Jiang, L.; Wu, X.-S.; Li, M.-L.; Ding, Q.; Wang, X.-a.; et al. Ursolic acid induces cell cycle arrest and apoptosis of gallbladder carcinoma cells. *Cancer Cell Int* **2014**, *14*, 96. doi:10.1186/s12935-014-0096-6.
24. Zhang, Y.; Ma, X.; Li, H.; Zhuang, J.; Feng, F.; Liu, L.; Liu, C.; Sun, C. Identifying the effect of ursolic acid against triple-negative breast cancer: Coupling network pharmacology with experiments verification. *Front Pharmacol* **2021**, *12*, 685773. doi:10.3389/fphar.2021.685773.
25. Kim, S.H.; Ryu, H.G.; Lee, J.; Shin, J.; Harikishore, A.; Jung, H.Y.; Kim, Y.S.; Lyu, H.N.; Oh, E.; Baek, N.I; Choi, K.Y. Ursolic acid exerts anti-cancer activity by suppressing vaccinia-related kinase 1-mediated damage repair in lung cancer cells. *Sci Rep* **2015**, *5*,14570. doi: 10.1038/srep14570.
26. Park, C.; Jeong, J.W.; Han, M.H.; Lee, H.; Kim, G.Y.; Jin, S.; Park, J.H.; Kwon, H.J.; Kim, B.W.; Choi, Y.H. The anti-cancer effect of betulinic acid in u937 human leukemia cells is mediated through ROS-dependent cell cycle arrest and apoptosis. *Anim Cells Syst (Seoul)* **2021**, *25*, 119-127. doi:10.1080/19768354.2021.1915380.
27. Goswami, P.; Paul, S.; Banerjee, R.; Kundu, R.; Mukherjee, A. Betulinic acid induces DNA damage and apoptosis in SiHa cells. *Mutat Res Genet Toxicol Environ Mutagen* **2018**, *828*, 1-9. doi:https://doi.org/10.1016/j.mrgentox.2018.02.003.
28. Wang, C.; Youle, R.J. The role of mitochondria in apoptosis. *Annu Rev Genet* **2009**, *43*, 95-118. doi:10.1146/annurev-genet-102108-134850.
29. Wei, J.; Liu, M.; Liu, H.; Wang, H.; Wang, F.; Zhang, Y.; Han, L.; Lin, X. Oleanolic acid arrests cell cycle and induces apoptosis via ROS-mediated mitochondrial depolarization and lysosomal membrane permeabilization in human pancreatic cancer cells. *J Appl Toxicol* **2013**, *33*, 756-765. doi:10.1002/jat.2725.
30. Hearps, A.C.; Burrows, J.; Connor, C.E.; Woods, G.M.; Lowenthal, R.M.; Ragg, S.J. Mitochondrial cytochrome c release precedes transmembrane depolarisation and caspase-3 activation during ceramide-induced apoptosis of Jurkat T cells. *Apoptosis* **2002**, *7*, 387-394. doi:10.1023/A:1020034906200.
31. Sánchez-Alcázar, J.A.; Khodjakov, A.; Schneider, E. Anti-cancer drugs induce increased mitochondrial cytochrome c expression that precedes cell death. *Cancer Res* **2001**, *61*, 1038-1044.
32. Bhadra, K. A mini review on molecules inducing caspase-independent cell death: A new route to cancer therapy. *Molecules* **2022**, *27*, 6401. doi: 10.3390/molecules27196401.
33. Di Meo, S.; Reed, T.T.; Venditti, P.; Victor, V.M. Role of ROS and RNS sources in physiological and pathological conditions. *Oxid Med Cell Longev* **2016**, *2016*, 1245049. doi:10.1155/2016/1245049.
34. Redza-Dutordoir, M.; Averill-Bates, D.A. Interactions between reactive oxygen species and autophagy: Special issue: Death mechanisms in cellular homeostasis. *Biochimica et Biophysica Acta (BBA) – Mol Cell Res* **2021**, *1868*, 119041. doi:10.1016/j.bbamcr.2021.119041.
35. Ling, T.; Boyd, L.; Rivas, F. Triterpenoids as reactive oxygen species modulators of cell fate. *Chem Res Toxicol* **2022**, *35*, 569-584. doi:10.1021/acs.chemrestox.1c00428.
36. Liby, K.; Honda, T.; Williams, C.R.; Risingsong, R.; Royce, D.B.; Suh, N.; Dinkova-Kostova, A.T.; Stephenson, K.K.; Talalay, P.; Sundararajan, C.; et al. Novel semisynthetic analogues of betulinic acid with diverse cytoprotective, antiproliferative, and proapoptotic activities. *Mol Cancer Ther* **2007**, *6*, 2113-2119. doi: 10.1158/1535-7163.MCT-07-0180.
37. Lewinska, A.; Adamczyk-Grochala, J.; Kwasniewicz, E.; Deregowska, A.; Wnuk, M. Ursolic acid-mediated changes in glycolytic pathway promote cytotoxic autophagy and apoptosis in phenotypically different breast cancer cells. *Apoptosis* **2017**, *22*, 800-815. doi:10.1007/s10495-017-1353-7.
38. Seo, J.; Jung, J.; Jang, D.S.; Kim, J.; Kim, J.H. Induction of cell death by betulinic acid through induction of apoptosis and inhibition of autophagic flux in microglia BV-2 cells. *Biomol & Ther* **2017**, *25*, 618-624. doi:10.4062/biomolther.2016.255.
39. Zhang, Y.; He, N.; Zhou, X.; Wang, F.; Cai, H.; Huang, S.H.; Chen, X.; Hu, Z.; Jin, X. Betulinic acid induces autophagy-dependent apoptosis via Bmi-1/ROS/AMPK-mTOR-ULK1 axis in human bladder cancer cells. *Aging (Albany NY)* **2021**, *13*, 21251-21267. doi:10.18632/aging.203441.
40. Yun, C.W.; Lee, S.H. The roles of autophagy in cancer. *Int J Mol Sci* **2018**, *19*. doi:10.3390/ijms19113466.
41. Liu, Z.; Yu, X.; Xu, L.; Li, Y.; Zeng, C. Current insight into the regulation of PD-L1 in cancer. *Exp Hematol Oncol* **2022**, *11*, 44. doi:10.1186/s40164-022-00297-8.
42. Pandey, M.K.; Sung, B.; Aggarwal, B.B. Betulinic acid suppresses STAT3 activation pathway through induction of protein tyrosine phosphatase SHP-1 in human multiple myeloma cells. *Int J Cancer* **2010**, *127*, 282-292. doi:10.1002/ijc.25059.
43. Kutkowska, J.; Strzadala, L.; Rapak, A. Sorafenib in combination with betulinic acid synergistically induces cell cycle arrest and inhibits clonogenic activity in pancreatic ductal adenocarcinoma cells. *Int J Mol Sci* **2018**, *19*, 3234. https://doi.org/10.3390/ijms19103234.

44. Kang, D.Y.; Sp, N.; Lee, J.M.; Jang, K.J. Antitumor effects of ursolic acid through mediating the inhibition of STAT3/PD-L1 signaling in non-small cell lung cancer cells. *Biomedicines* **2021**, *9*, doi:10.3390/biomedicines9030297.
45. Torres-Martinez, Z.; Pérez, D.; Torres, G.; Estrada, S.; Correa, C.; Mederos, N.; Velazquez, K.; Castillo, B.; Griebenow, K.; Delgado, Y. A synergistic pH-responsive serum albumin-based drug delivery system loaded with doxorubicin and pentacyclic triterpene betulinic acid for potential treatment of NSCLC. *BioTech (Basel)* **2023**, *12*. doi:10.3390/biotech12010013.